Multifractal dimension and *b* value analysis of the 1998–1999 Quito swarm related to Guagua Pichincha volcano activity, Ecuador

D. Legrand[1,2]
Institut Français d'Etudes Andines, Quito, Ecuador

D. Villagómez,[1,3] H. Yepes,[1] and A. Calahorrano[1,4]
Instituto Geofísico de la Escuela Politécnica Nacional, Quito, Ecuador

Received 6 May 2003; revised 20 October 2003; accepted 13 November 2003; published 24 January 2004.

[1] Temporal variations of spatial multifractal dimensions of Quito swarm seismicity (Ecuador) are related to the August 1998 to December 1999 Guagua Pichincha volcanic activity. Multifractal dimensions decrease a few days before the five main seismic energy peaks and increase again before or just after these peaks. This behavior reveals a self-organization of earthquakes that precedes main seismic energy peaks. The Quito swarm is also characterized by a bimodal Gutenberg-Richter law with two ***b*** values: b_1 = 0.95 ± 0.15 and b_2 = 1.48 ± 0.15. This bimodality may reveal the superposition of two different processes: one related to a classical elastic rupture and the other related to hydraulic fracture (leading to high *b* values) resulting from magma and overpressurized groundwater movements. Groundwater expulsion may be driven by heat released from deeper upgoing magma and manifested on the surface by the occurrence of phreatic explosions (beginning 7 August 1998) and by the formation of eight dacitic lava domes (beginning 25 September 1999). *INDEX TERMS:* 7209 Seismology: Earthquake dynamics and mechanics 7215 Seismology: Earthquake parameters; 7223 Seismology: Seismic hazard assessment and prediction; 7260 Seismology: Theory and modeling; 7280 Seismology: Volcano seismology (8419); *KEYWORDS:* volcanic swarm, Guagua Pinchincha, *b* value, multifractal

Citation: Legrand, D., D. Villagómez, H. Yepes, and A. Calahorrano (2004), Multifractal dimension and *b* value analysis of the 1998–1999 Quito swarm related to Guagua Pichincha volcano activity, Ecuador, *J. Geophys. Res.*, *109*, B01307, doi:10.1029/2003JB002572.

1. Introduction

[2] A swarm of tectonic-like high frequency (1–10 Hz) events with clear *P* and *S* waves appeared in two separate episodes before the 1998–1999 phreatic and magmatic activity periods of Guagua Pichincha volcano (GPV), Ecuador [*Calahorrano et al.*, 1999; *Calahorrano*, 2001; *Legrand et al.*, 2002]. This swarm was located in the northern part of the city of Quito, about 15 km NE of the volcano (Figure 1). The first episode started in July 1998, one month before a period of intense phreatic activity of GPV. A second, less energetic episode occurred in June–August 1999, 2 months before the magmatic activity of GPV, which started in September 1999 with the extrusion of dacitic domes and volcanic events below the volcanic vent [*Villagómez et al.*, 1999; *Villagómez*, 2000]. A M_w = 7.1 subduction earthquake occurred on 4 August 1998, at 1859 UT, in Bahía de Caráquez (200 km west of GPV, Figure 1) few weeks after the beginning of the Quito swarm. It occurred 3 days before the beginning of a period of intense phreatic activity, which included hundreds of phreatic explosions [*Villagómez*, 2000; *Segovia*, 2001]. As this event is strongly correlated with GPV in space and time, and as the volcano had started a slow phreatic reactivation since 1981, it may have been a catalyzer of the intense phreatic and magmatic activity, even if it can not be proved. This article will focus on the description and the understanding of the volcanic complex dynamics by the study of *b* values and temporal variations of spatial multifractal dimensions D_q.

[3] A swarm is defined as a large number of small seismic events with respect to large events (i.e., there is not a predominant main event) that are concentrated in space and time [*Mogi*, 1963]. The *b* value of swarm-like seismic activity is often significantly higher than typical tectonic average values, which vary from 0.67 to 1.0 [*Gutenberg and Richter*, 1949, 1954; *Lay and Wallace*, 1995]. Furthermore, b-values are commonly larger in volcanic regions than in tectonic ones [*Francis*, 1968a, 1968b]. Some examples are the 1.3 *b* value at the northern Mid-Atlantic Ridge [*Sykes*, 1970]; 1.24 for the 1968 Fernandina caldera collapse in the volcanic Galapagos Islands, Ecuador [*Francis*, 1974]; 1.2 ±

[1]Also at Instituto Geofísico de la Escuela Politécnica Nacional, Quito, Ecuador.
[2]Now at Departamento de Geofísica (DGF), Universidad de Chile, Santiago, Chile.
[3]Now at Department of Geological Sciences, University of Oregon, Eugene, Oregon, USA.
[4]Now at Géosciences Azur, Villefranche-sur-Mer, France.

0148-0227/04/2003JB002572$09.00

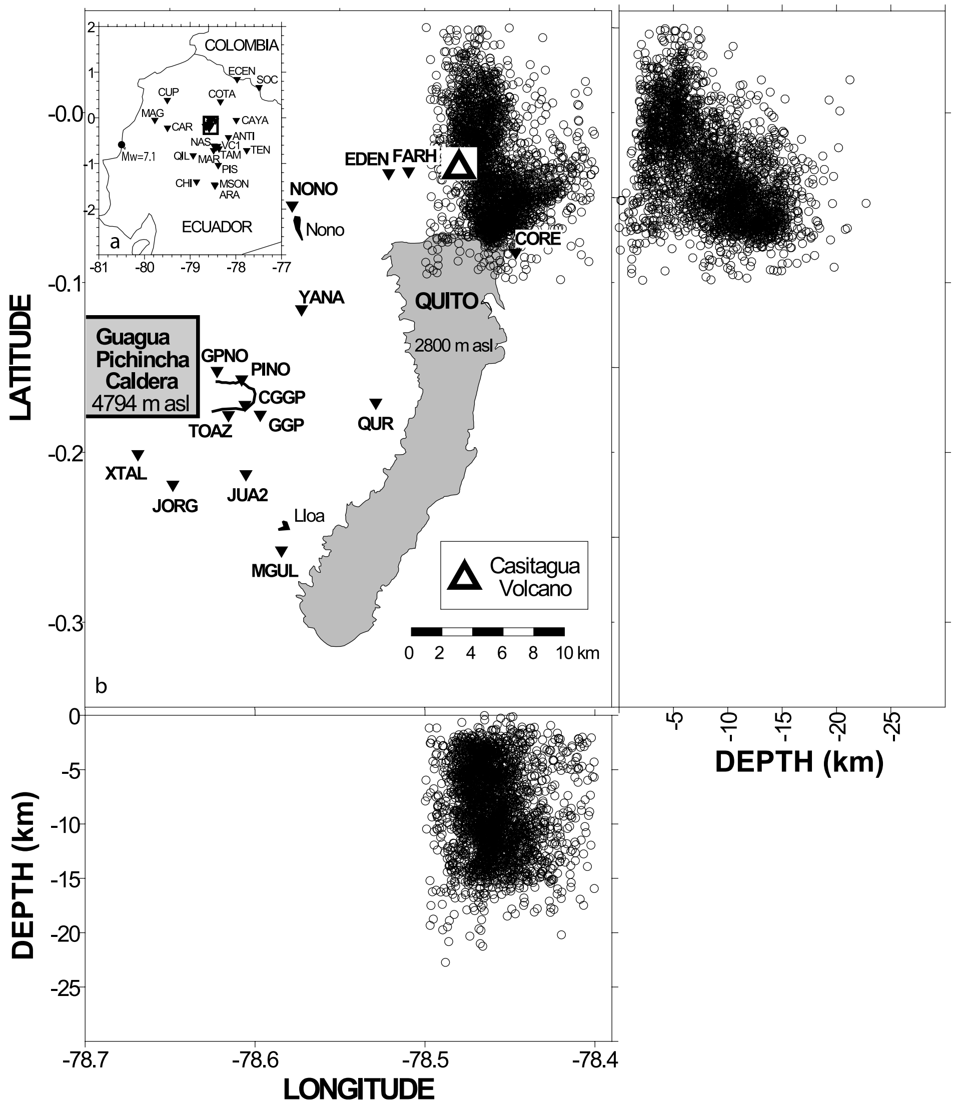

Figure 1. Regional and local seismic stations (triangles) used to locate the Quito swarm earthquakes. The events were located using the Master Event method [*Spence*, 1980; *Besse*, 1986].

0.1 for the 1989 Mammoth Mountain volcano swarm, California [*Hill et al.*, 1990]; 1.2 for the 1989 off Eastern Izu Peninsula swarm, Japan, associated to a submarine volcanic eruption [*Matsumura et al.*, 1991]; and greater than 1.3 at Mount St. Helens volcano [*Wiemer and McNutt*, 1997]. Nevertheless, high *b* values are not exclusive of volcanic regions. For example, a *b* value of 1.3 ± 0.1, with a 98% of confidence has been calculated for Bucaramanga swarm, Colombia [*Rivera*, 1989]. High *b* values (1.2 ± 0.11 for depth <4 km and 1.28 ± 0.12 around 4-km depth) have been found in shallow parts of the Parkfield segment of the San Andreas Fault [*Wiemer and Wyss*, 1997].

[4] Spatial and temporal *b* value variations have been observed before large earthquakes [e.g., *Suyehiro et al.*, 1964; *Mogi*, 1969; *Smith*, 1981; *Wyss and Habermann*, 1988] and around volcanoes [*Wyss et al.*, 1997; *Wiemer and McNutt*, 1997; *Wiemer et al.*, 1998; *Power et al.*, 1998]. The separation of spatial and temporal aspects in such studies is a big challenge. When performing three-dimensional tomographic analysis of *b* values, especially on small cells, it is difficult to ensure that the Gutenberg-Richter (GR) law is respected, i.e., that different sizes of earthquakes will be well sampled in each cell (exclusion of large events in many small spatial cells leads to artificially high *b* values). In this article, all of the earthquakes included in the whole region are considered, without solving the space and time interaction problem (see section 4).

[5] The complexity of spatial distributions of earthquakes cannot always be described by a single parameter, such as the *b* value or one fractal dimension *D* [e.g., *Kagan and Knopoff*, 1978; *Ogata*, 1988; *Hirata*, 1989]. It is sometimes necessary to calculate a spectrum of multifractal dimensions, which may describe better this complexity [e.g., *Hirata and Imoto*, 1991; *Dongsheng et al.*, 1994]. We will show that the Quito swarm and the corresponding Guagua Pichincha volcanic activity are not simply linear processes but are complex and must be described by nonlinear physics.

2. Seismic Network and Earthquake Locations

[6] The seismic network used for this study is composed of 35 short-period (one and three component) stations, with

15 stations close to the swarm (Figure 1). Event locations must be very precise because slight location errors may overestimate spatial multifractal dimensions [*Kagan and Knopoff*, 1980; *Eneva*, 1996]. The master event technique [*Spence*, 1980; *Besse*, 1986] allows a more precise determination of hypocentral locations. However, this technique only calculates relative hypocenters with respect to a reference earthquake. However, as multifractal dimension calculations are not sensitive to absolute locations, an error in the reference earthquake location will not affect the results.

[7] Events comprising a swarm mainly occur within a small spatial region; hence some of their waveforms may have a similar shape. These events with similar waveforms, called multiplets, are thought to have a common focal mechanism [*Poupinet et al.*, 1984]. They used this waveform similarity of earthquakes in the Calaveras fault, California, to do a relative relocation of events with respect to a well-known hypocenter location. However, even though some of the events of the Quito swarm can be recognized as multiplets, not all of them have the same focal mechanism [*Legrand et al.*, 2002]. Therefore hypocenter locations were not determined using the multiplet technique. Instead, relocations were performed with the master event technique to accommodate the complete catalogue of events.

[8] Local magnitudes have been calculated using the duration T (s) of the seismogram with a classical formula [*Lee et al.*, 1972]: $M_L = -0.87 + 2.0 * \log_{10}T + 0.0035*\Delta$, where Δ is the epicentral distance (km). Event durations were determined using seismic records from station QUR when available, or the closest stations when QUR was not functioning.

3. Catalogue Compilation

[9] Determination of temporal variations of seismic parameters requires a complete catalogue over time and careful examination of the acquisition conditions of the data. Correlation between temporal variations of a parameter with any change of its acquisition conditions may be considered as suspect. For example, finding a double slope in GR law is always a priori suspicious, and much attention must be taken in order to be sure that this break is real [*Main*, 2000]. Artificial changes in the rates of seismic activity related to changes in the seismic network configuration (installation, change or closure of seismometers, change in instrument gains, change in the magnitude thresholds of complete recording, change in the way of calculating the magnitude, etc.) may affect *b* value calculations over time [*Habermann*, 1987; *Eneva et al.*, 1994]. For example, there were two slopes in the GR law in Long Valley caldera, California, during intense swarm activity [*Barton et al.*, 1999]. Barton et al. explain this artificial break by the lack of small event readings during the period of intense seismic activity. In this case, the *b* value of intense activity corresponding to the segment of large events is similar to the *b* value for a complete catalogue corresponding to low levels of activity. In contrast, the *b* value corresponding to the segment of small events is artificially low due to incomplete cataloguing of events during intense seismic activity, and is smaller than the *b* value corresponding to a complete catalogue for the same magnitude range during normal seismic activity.

4. The *b* Values of Quito Swarm

[10] There is a duality between space and time in *b* value calculations. This means that if a complete description of the GR law is expected (i.e., there is a linear part of this law), one must consider a small region over a long time (t) of observation, or a greater region over a smaller time interval. Hence spatial and temporal windows cannot be chosen independently. If the maximum magnitude recorded in the region is $M_{\max}$, the size of the region over which the *b* value is calculated should be at least equal to the characteristic size of the earthquake of magnitude $M_{\max}$, to be sure to record all the aftershocks associated with the main shock. Once the spatial window is taken, the temporal window should be long enough that all magnitude ranges are sampled during this time window. If the space is divided into small cells, it is not certain that each cell will have the same number of events. Hence the GR law may not be equally representative in space and may not be applied in cells with few data points.

[11] Beneath a volcano, we usually consider a small region, so theoretically a long time window interval should be taken, to be sure to record all the significant activity (especially large events) of that region. This condition is rarely satisfied, because large events rarely occur beneath volcanoes. However, exceptions exist; large earthquakes have been recorded close to some volcanoes, for example: $M_s = 7.1$ in 1975 close to Kalapana volcano (United States), $M = 7.0$ in 1912 close to Katmai volcano (United States), and $M_s = 7.0$ in 1914 at Sakura-jima volcano (Japan). So high *b* value estimates under a volcano may, in some particular cases, be due to an artifact of a small time window. Additionally, it is almost impossible to calculate temporal variations of *b* values of a swarm in short time windows. The *b* value calculation requires a distribution of large and small events in such a way that the GR law is satisfied (i.e., presence of a linear part over a finite magnitude range). It may be necessary to consider a long time window to correctly and completely sample large and small events of a swarm due to the nearly random distribution of large and small events with time. Hence we calculate *b* values for the whole volume where events occurred and for the entire period from March 1998 to December 1999.

5. Double Slope in the GR Law of Quito Swarm: Real or Not?

[12] The *b* value of the GR law was calculated with the maximum likelihood method. For the case of single slope (Figure 2c) we use the method of *Aki* [1965], and for the case of a double slope (Figures 2a and 2b) we use the method of *Shimazaki* [1986] for which a conversion from magnitude to seismic moment was done in order to achieve a log-log relation. The Quito swarm is characterized by a GR law with two *b* values: $b_1 = 0.95 \pm 0.15$ and $b_2 = 1.48 \pm 0.15$ (Figure 2b).

[13] One possible explanation for the source of double slopes in GR laws is that changes in the configuration of the seismic network introduce artifacts in the GR law. For the

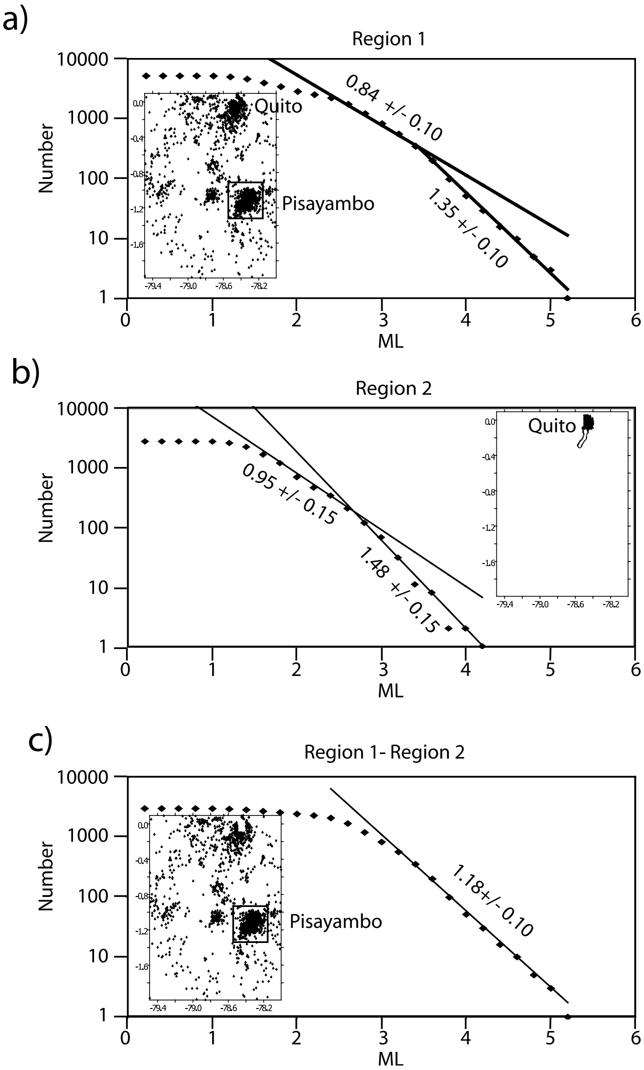

Figure 2. Gutenberg-Richter law with respect to local magnitude, corresponding to seismicity from March 1998 to December 1999 for (a) region 1, Quito swarm and surrounding areas, (b), region 2, Quito swarm only, and (c) region 1–region 2. Squares in a and c correspond to the nonvolcanic Pisayambo swarm.

Quito swarm, two new stations (FARH and EDEN) were installed close to the epicenters after the beginning of the swarm (Figure 1). These two new stations allowed a better precision in event locations. Nevertheless, these installations have not affected the number of events of magnitude >1.4 (the magnitude threshold) that could be recorded by the 13 other nearby stations. Hence the double slope observed is not an artifact of changes in the seismic network.

[14] The validity of the double slope was determined using the following steps:

[15] 1. The GR law was calculated for a large region that includes the Quito swarm (Figure 2a). A double slope in the GR law was observed: the first one with a *b* value of 0.84 ± 0.1 between M_L = 2.5 and 3.4 and the second one with a *b* value of 1.35 ± 0.1 between M_L = 3.4 and 5.2. This suggests that two different processes (corresponding to two slopes) are the source of seismicity in this area.

[16] 2. The *b* values were also calculated for the Quito swarm alone (Figure 2b). The double slope is still observed, one with a *b* value of 0.95 ± 0.15 between magnitude M_L of 1.4 and 2.6, and another one with a *b* value of 1.48 ± 0.15 between M_L = 2.6 and 4.2.

[17] 3. Finally, the GR law was calculated for region 1–region 2 (Figure 2c). We observe only one slope with a *b* value of 1.18 ± 0.1 between M_L = 3.2 (the regional threshold magnitude) and 5.2. This value is close to that of the Quito swarm for magnitudes between 1.5 and 2.6 (Figure 2b, first slope) and is close to the typical *b* value of about 1.0 and may be considered as the regional *b* value. One could think that the double slope of the entire area (step 1) is related to another swarm. The data shows a second swarm, nonvolcanic, called the Pisayambo swarm (Figures 2a and 2c). However, Figure 2c includes the Pisayambo swarm but does not show a double slope. Therefore we attribute the double slope exclusively to the Quito swarm.

6. D_q Values of the Quito Swarm

[18] In order to deal with a complete catalogue, we only take into account events with a magnitude greater than or equal to the threshold magnitude of complete recording (linear parts of the GR law). To remain consistent in our analysis, we use the same catalogue of events (M_L > 1.4), where a double *b* value is observed, to determine D_q values.

[19] D_q values and *b* values cannot be calculated over the same time windows because, while *b* values must be calculated over a wide range of magnitudes (i.e., over a long time window), D_q values do not take magnitude into account (i.e., a smaller time window can be used). Temporal evolution of D_q values is performed on sliding windows of 200 events with an overlap of 20. These numbers have been chosen empirically so that for each sliding window enough points exist to calculate D_q values. This is accomplished by visually inspecting each graph. Moreover, D_q values were calculated for the entire data set and compared to a sliding window, where no variation was expected. The minimum number of events necessary to describe the D_q values of the entire data set was tested empirically, using different lengths of the sliding window. This method is based on the assumption that a subset of another fractal set is a fractal set with the same fractal dimension. The bias that may be introduced is considered to be constant over time. Therefore, in many cases, using the entire data set available does not imply a better resolution [*Eneva*, 1996]. Here, the study was limited to a complete data set in magnitude corresponding to the linear parts of the GR law. However, an infinite data set should be used to be sure of the multifractal behavior. In the case of a limited data set, a monofractal set can appear as multifractal [*Havstad and Ehlers*, 1989; *Eneva*, 1996]. In order to show a multifractal behavior, an infinite number of points should be used. It is impossible on real data, and as a consequence a real multifractal behavior often appears as monofractal [*Eneva*, 1996]. As a result, we will focus on the temporal variations of D_q values, not the multifractal characteristic of the data set. Temporal variations in D_q values can provide a powerful tool for detecting large seismic activity, as have been demonstrated in laboratory rock failure experiments [*Hirata et al.*, 1987], large earthquakes [*Radulian and Trifu*, 1991],

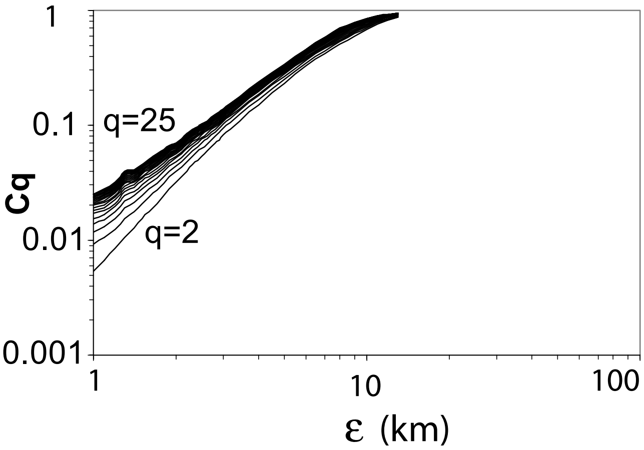

Figure 3. Example of correlation function C_q versus ε in km for period 1, with q varying from $q = 2$ to $q = 25$.

mine earthquakes [*Coughlin and Kranz*, 1991; *Eneva*, 1996], synthetic catalogs [*Eneva and Ben-Zion*, 1994], and aftershock sequences [*Legrand et al.*, 1996].

[20] There are many fractal dimension definitions and descriptions [*Eckmann and Ruelle*, 1985; *Baker and Gollub*, 1990] (few of them are summarized by *Legrand et al.* [1996]). For example, the capacity dimension D_C

$$D_C = \lim_{\varepsilon \to 0} \frac{\log_{10} N(\varepsilon)}{\log_{10}(1/\varepsilon)}$$

where $N(\varepsilon)$ is the number of filled boxes of size ε needed to cover the fractal object, often called the "box-counting" method.

[21] The information dimension D_I:

$$D_I = \lim_{\varepsilon \to 0} \frac{I(\varepsilon)}{\log_{10} \varepsilon} = \lim_{\varepsilon \to 0} \frac{\sum_{i=1}^{N} p_i \log_{10} p_i}{\log_{10} \varepsilon}$$

where $p_i = p_i(\varepsilon)$ is the probability of occupation of the ith box of size ε, $S(\varepsilon) = -I(\varepsilon) = -\sum_{i=1}^{N} p_i \log_{10} p_i$ is the entropy (minus the information $I(\varepsilon)$), and N is the number of boxes. The information dimension takes into account the number of points in each box that the capacity dimension does not account for.

[22] The correlation dimension D_G:

$$D_G = \lim_{\varepsilon \to 0} \frac{\log_{10} C(\varepsilon)}{\log_{10} \varepsilon}$$

where

$$C(\varepsilon) = \frac{1}{N} \sum_{j=1}^{N} \left[\frac{1}{N-1} \sum_{\substack{i=1 \\ i \neq j}}^{N} H\left(\varepsilon - \| \underline{x}_i - \underline{x}_j \|\right) \right]$$

is the correlation function, N is the number of points, $\|\underline{x}_i - \underline{x}_j\|$ is the distance between the two points x_i and x_j, and H is the Heaviside function. This definition takes into account the spatial distribution of points inside each box and was first introduced by *Grassberger and Procaccia* [1983] for a temporal signal, generalized afterward for a spatial set of points.

[23] The generalized fractal dimensions D_q:

$$D_q = \frac{1}{q-1} \lim_{\varepsilon \to 0} \frac{\log_{10} \left(\sum_{i=1}^{N(\varepsilon)} p_i^q \right)}{\log_{10}(\varepsilon)}$$

defined by *Grassberger* [1983] and *Hentschet and Procaccia* [1983], where $p_i = p_i(\varepsilon)$ is the probability of occupation of the ith box of size ε and q is a positive or negative real number. This definition takes into account the generalization distance of order q between points, and can be seen as a generalization of order q of the correlation dimension. The parameter p_i^q is the probability of having q points within the ith box, so q can be interpreted as the degree of correlation. D_q can be calculated in a similar way as the correlation dimension [*Kurthz and Herzel*, 1987; *Hirata and Imoto*, 1991; *Eneva*, 1994]:

$$D_q = \lim_{\varepsilon \to 0} \frac{\log_{10} C_q(\varepsilon)}{\log_{10} \varepsilon}$$

with

$$C_q(\varepsilon) = \left\{ \frac{1}{N} \sum_{j=1}^{N} \left[\frac{1}{N-1} \sum_{\substack{i=1 \\ i \neq j}}^{N} H\left(\varepsilon - \| \underline{x}_i - \underline{x}_j \|\right) \right]^{(q-1)} \right\}^{\frac{1}{q-1}}$$

We have the following properties: $D_0 = D_C$, $D_1 = D_I$ and $D_2 = D_G$ and D_q is a decreasing function of q, i.e., if $p < q$, then $D_p > D_q$. For a simple monofractal, D_q is independent of q and all these definitions are equal.

[24] All these definitions express geometry only (i.e., number of earthquakes within boxes independent of magnitude), so we assume a self-similarity of events with respect to magnitude. A simple model of a point source is also assumed for each event, independent of the magnitude. A more accurate analysis would account for fault plane orientation and size, however, we do not take this into account because focal mechanisms are not known well enough in this study.

[25] For each window, the correlation function, C_q, was determined for different values of ε for $q = 2$ to $q = 25$ (period 1 is shown in Figure 3). The temporal variation of D_q values show at least 5 peaks, which are consistent from $q = 2$ to $q = 25$ (Figure 4). The multifractal spectrum, the change in D_q as a function of q, shows that as q increases D_q decreases toward the constant value D (Figure 5).

[26] Temporal variations of multifractal dimension D_2 are compared to earthquake energy (Figure 6). Only D_2 is shown for clearness. The multifractal dimensions decrease a few days before the five main energy peaks of activity. After the decrease, the dimensions increase and come back to their original value before or just after the maximum energy peak. Peaks 4 and 5 are close, indicating that D_2 did not have time to return to its initial value. Nearly constant multifractal dimensions describe the quiescence period between peaks 2 and 3. Note that the lengths of the time windows are not constant (Figure 6, top).

7. Discussion

7.1. Closed/Open System

[27] The Gutenberg-Richter law has widely been verified for tectonic main shock/aftershock sequences, with classical

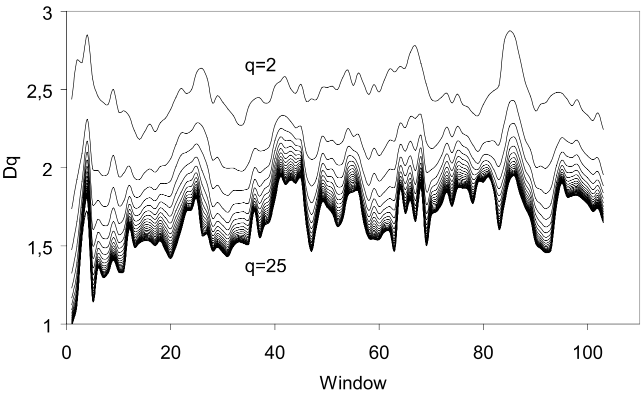

Figure 4. Multifractal dimensions D_q for q varying from q = 2 to q = 25 versus all temporal windows.

b values close to 1.0. When a large earthquake occurs, the elastic medium reacts to this excitation without any other outside force, and aftershocks occur re-organizing themselves with respect to the main magnitude, following a time decay described by Omori's law. Such a system can be called a closed system, because there is no external energy brought in it. A volcanic system is different. Additional energy may be introduced (e.g., thermal energy generated by magma, overpressurized water or gas), generating a thermoelastic stress [*Warren and Latham*, 1970]. Therefore a volcanic system may be described as an open system. Substantial external energy can enter the system, leading to the generation of many small events, without generating a large main shock as observed for tectonic earthquakes. In this case, a high b value will be obtained.

[28] These closed/open systems can be inferred from seismogram forms. For a typical earthquake, the seismogram shows an impulsive beginning of P waves followed by a decay of amplitude with time. This signal indicates a free response of the ground to the short impulse responsible for the earthquake. In the case of volcanic events (tremor, phreatic, and/or magmatic explosions), the seismic signal is completely different. The signal does not show a regular decay of amplitude with time; amplitude may remain constant for long periods of time such as in volcanic tremor. Phreatic explosions often appear as long and complicated signals that represent the superposition of many small elementary and simple events. Signal without regular decay periods suggest that the medium does not respond to a single triggering force, but to a sustained excitation of the source. On the basis of an analogy between a single event and a swarm, we conclude that a swarm is not the response of a single excitation, like a large event followed by many aftershocks, but is due to the result of sustained source excitation (i.e., movement of over pressurized fluids, stress changes, etc).

[29] High b values ($\gg$1) reflect a high occurrence of small events with respect to large events. Different explanations for this have been proposed. *Mogi* [1962] suggested that highly heterogeneous materials submitted to mechanical loading might generate high b values. *Scholz* [1968] and *Wyss* [1973] proposed that high b values are probably related to a decrease in the amplitude of the stress applied to the sample, which is accompanied by smaller fractures. The b value may be somewhat related to the nature of the rocks: a ductile rock has a higher b value than a brittle rock [*Scholz*, 1968]. Scholz showed that variations in b values were also related to the porosity of a rock: In highly porous rock, the proportion of microfractures is greater than in a less porous rock, therefore the b value will be higher. For volcanoes, small earthquakes are usually recorded often occurring along small faults. Furthermore, volcanic rocks are commonly porous. Elevated fluid pressure decreases the effective normal stress facilitating microcrack formation, which leads to high b values [*Scholz*, 1968] as in reservoir-induced seismicity [*Simpson et al.*, 1988]. *Warren and Latham* [1970] showed on sample experiments that thermoelastic stresses due to thermal gradients might also lead to b values significantly larger than 1, as often observed in volcanoes. Warren and Latham observed that seismic activity on samples starts abruptly, immediately after a thermal gradient was applied, and the maximum of activity corresponds roughly to the maximum of the thermal gradient. They also observed the presence of swarms after the apparent end of activity, correlated with small fluctuations in the thermal gradient.

7.2. Lack of Large Events and Corresponding GR Law Break

[30] Gutenberg-Richter law breaks have been described for large events [*Scholz*, 1982; *Pacheco et al.*, 1992]. These breaks can be explained by the finite thickness of the seismogenic lithosphere, which limits the rupture zone width. The only possibility for a large fault is an extension in a horizontal direction [*Scholz*, 1982; *Pacheco et al.*, 1992]. Since, in the case of the Quito swarm, only small events (M_L < 4.2) are involved, we can assume that faults grew with a self-similar pattern (i.e., square and not rectangular). Therefore the break in the Gutenberg-Richter law must be explained by another hypothesis.

7.3. Multifractal Dimension

[31] A temporal evolution of b value is difficult to achieve in the case of a swarm because a large number of events is required. A good alternative is to use a multifractal study for which a smaller number of events is sufficient. The complexity of the spatiotemporal self-organization of events is due to fundamental physical processes that are not completely understood, as suggested by *Sornette and Sornette* [1999] and *Wesnousky* [1999].

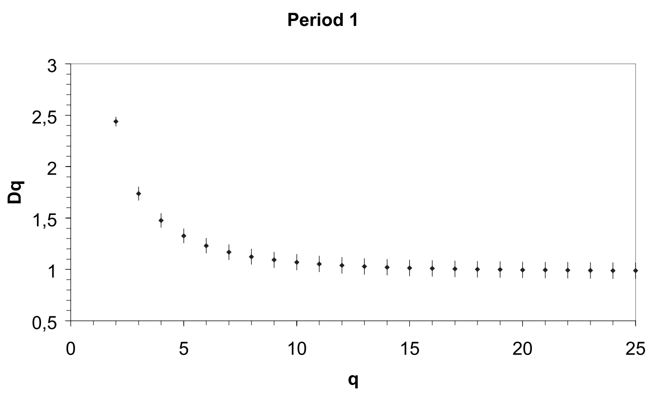

Figure 5. Example of a multifractal spectrum of D_q versus q for q = 2 to 25, for period 1. As q is increasing, D_q is decreasing toward the limit constant value D_∞.

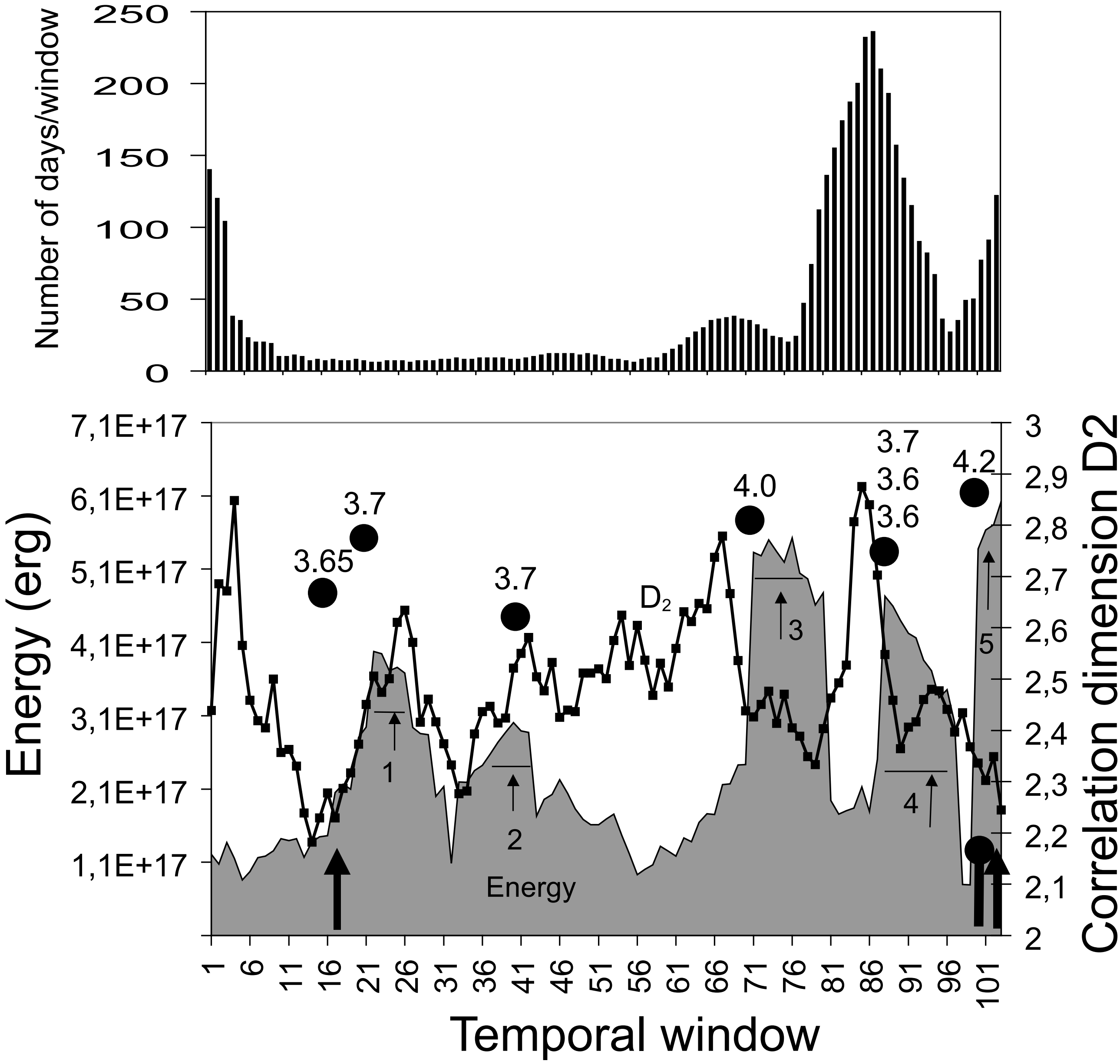

Figure 6. Temporal variations of energy (shaded area) and multifractal dimension D_2 (heavy line). The eight largest earthquake magnitudes are shown (black points). The two vertical arrows correspond to the first phreatic explosion (in period 17) and the large phreatic explosions of 5 and 7 October 1999 (period 102). The vertical line with a dot corresponds to the extrusion of the first lava dome on 25 to 30 September 1999 (periods 99 and 100).

[32] A break in fractal dimensions has already been shown during fluid extraction [*Volant et al.*, 1992]. In our study, we only observe a break in the GR law and not in the multifractal dimension analysis. This difference is attributed to the fact that the number of events involved in the break of the GR law correspond to a small percentage of events ($2.7 < M_L < 5.2$), too few to affect multifractal spatial dimensions.

8. Conclusions

[33] The two episodes of the Quito swarm are an unusual case of volcano-related seismicity as they are located 15 km from an active volcano. These events are located in the northern part of the city, beneath the old Casitagua volcanic complex (Figure 1), where many preexisting small faults probably exist and where an active reverse fault system is located. Casitagua volcano is extinct and the distance to GPV is large enough (15 km from the swarm epicentral zone) that the thermal stress hypothesis for high *b* values does not seem probable. In 1998, the Quito swarm activity began 2 months before the first phreatic explosion of 7 August, and in 1999, the second peak occurred 2 months before the onset of magmatic activity on 25 September [*Calahorrano*, 2001; *Legrand et al.*, 2002]. The slow rise of magma is accompanied by overpressured groundwater that generates the first episode of the Quito swarm and the first phreatic

explosions at GPV. In this case, magma movements and corresponding overpressurized water and/or gas ejection are likely to change the local stress regime, triggering the Quito seismic swarm.

[34] The Gutenberg-Richter law shows a clear double slope i.e., it has two different b values (Figure 2). We interpret this phenomenon as the superposition of two different physical processes. One is related to a classical elastic fracturation of the rocks with a classical b value close to 1 ($b_1 = 0.95 \pm 0.15$). The other is related to a hydraulic fracturation mechanism where faults can not reach high magnitudes because of overpressurized water and resultant increased normal stress. The lack of large magnitude events will produce a high b value $b_2 = 1.48 \pm 0.15$. Following the second episode of the Quito swarm, GPV was active; magmatic activity began two months later on September 1999. We suppose that while magma was ascending (beginning in July 1998) some overpressurized water was ejected, explaining the bimodal Quito swarm behavior.

[35] We show that multifractal dimensions decrease a few days before the five main energy peaks. In two cases they have time to come back to their initial value before the peak and in the other cases they come back afterward. A decrease and subsequent increase of multifractal dimensions had been shown before big aftershock sequences [*Legrand et al.*, 1996]. A similar behavior is shown here for activity close to a volcano. This may be useful in predicting short-term seismic energy peaks. Even if this behavior may not be used to predict any long-term volcanic explosion, we interpret it as temporal, non-long-term-predictable, chaotic dynamic behavior.

[36] **Acknowledgments.** We thank two anonymous reviewers for corrections made to this article. We thank the staff of the Geophysics Institute of Quito of the Escuela Politécnica Nacional for the monitoring and maintenance of the National network in Ecuador and the 24-hour surveillance during the 2-year crisis. We thank J. C. Ruegg for providing us with his code of Master Event Relocation. We thank also the IRD (Institut de Recherche pour le Développement), the IFEA (Institut Français d'Etudes Andines) and the MAE (French Ministère des Affaires Etrangères) for supporting a portion of this study. Thanks to Jean-Philippe Eissen for reading this article. Thanks to Heather Wright and Caroline for editing and valuable comments. Recuerdos sinceros al amigo Diego Viracucha quien tanto trabajó en el volcán Guagua Pichincha.

References

Aki, K. (1965), Maximum likelihood estimate of b in the formula log $N = a - bM$ and its confidence limits, *Bull. Earthquake Res. Inst. Univ. Tokyo*, *43*, 237–239.

Baker, G., and J. Gollub (1990), *Chaotic Dynamics: An Introduction*, Cambridge Univ. Press, New York.

Barton, D., G. Foulger, J. Henderson, and B. Julian (1999), Frequency-magnitude statistics and spatial correlation dimensions of earthquakes at Long Valley caldera, California, *Geophys. J. Int.*, *138*, 563–570.

Besse, P. (1986), Relocalisation relative d'événements sismiques appliqué à la région Sud du lac Ghoubbet situé dans la République de Djibouti, Ph.D. thesis, 49 pp., Jussieu Univ., Paris.

Calahorrano, A. (2001), Estudio del origen del enjambre sísmico de la zona norte de la ciudad de Quito, durante 1998–99, tesis de ingeniera geóloga, 190 pp., Escuela Politécn. Nac., Fac. de Geol., Minas y Petról., Quito, Ecuador.

Calahorrano, A., H. Yepes, B. Guillier, M. Ruiz, M. Segovia, M. Villagómez, and D. Andrade (1999), Seismic swarm in Quito (Ecuador): Tectonic or volcanic origin?, paper presented at Fourth International Symposium on Andean Geodynamics, Int. Lithosphere Program, Goettingen, Germany.

Coughlin, J., and R. Kranz (1991), New approaches to studying rock burst-associated seismicity in mines, *Proc. U.S. Rock Mech. Symp.*, *32nd*, 491–500.

Dongsheng, L., Z. Zhaobi, and W. Binghong (1994), Research into the multifractal of earthquake spatial distribution, *Tectonophysics*, *233*, 91–97.

Eckmann, J. P., and D. Ruelle (1985), Ergodic theory of chaos and strange attractors, *Rev. Mod. Phys.*, *57*, 617–656.

Eneva, M. (1994), Monofractal or multifractal: A case study of spatial distribution of mining induced seismic activity, *Nonlinear Processes Geophys.*, *1*, 182–190.

Eneva, M. (1996), Effect of limited data sets in evaluating the scaling properties of spatially distributed data: An example from mining-induced seismic activity, *Geophys. J. Int.*, *124*, 773–786.

Eneva, M., and Y. Ben-Zion (1994), Patterns in synthetic seismicity along faults undergoing brittle and creep deformations (abstract), *Eos Trans. AGU*, *75*(44), Fall Meet. Suppl., 462.

Eneva, M., R. Habermann, and M. Hamburger (1994), Artificial and natural changes in the rates of seismic activity: A case study of the Garm region, Tadjikistan (CIS), *Geophys. J. Int.*, *116*, 157–172.

Francis, T. (1968a), The detailed seismicity of mid-oceanic ridges, *Earth Planet. Sci. Lett.*, *4*, 39–46.

Francis, T. (1968b), Seismicity of mid-oceanic ridges and its relation to properties of the upper mantle and crust, *Nature*, *220*, 899–901.

Francis, T. (1974), A new interpretation of the 1968 Fernandina caldera collapse and its implications for the Mid-Oceanic ridges, *Geophys. J. R. Astron. Soc.*, *39*, 301–318.

Grassberger, P. (1983), Generalized dimensions of strange attractors, *Phys. Lett. A*, *97*, 227–230.

Grassberger, P., and I. Procaccia (1983), Measuring the strangeness of strange attractors, *Physica D*, *9*, 189–208.

Gutenberg, B., and C. Richter (1949), *Seismicity of the Earth and Associated Phenomena*, Princeton Univ. Press, Princeton, N. J.

Gutenberg, B., and C. Richter (1954), *Seismicity of the Earth and Associated Phenomena*, 2nd ed., Princeton Univ. Press, Princeton, N. J.

Habermann, R. (1987), Man-made changes of seismicity rates, *Bull. Seismol. Soc. Am.*, *77*, 141–159.

Havstad, J., and C. Ehlers (1989), Attractor dimension of nonstationary dynamical systems from small data sets, *Phys. Rev. A*, *39*, 845–853.

Hentschet, H., and I. Procaccia (1983), The infinite number of generalized dimensions of fractals and strange attractors, *Physica D*, *8*, 435–444.

Hill, D., W. Ellsworth, M. Johnston, J. Langbein, D. Oppenheimer, A. Pitt, P. Reasenberg, M. Sorey, and S. McNutt (1990), The 1989 earthquake swarm beneath Mammoth Mountain, California: An initial look at the 4 May through 30 September activity, *Bull. Seismol. Soc. Am.*, *80*, 325–339.

Hirata, T. (1989), A correlation between the b value and the fractal dimension of earthquakes, *J. Geophys. Res.*, *94*, 7507–7514.

Hirata, T., and M. Imoto (1991), Multifractal analysis of spatial distribution of micro-earthquakes in the Kanto region, *Geophys. J. Int.*, *107*, 155–162.

Hirata, T., T. Satoh, and K. Ito (1987), Fractal structure of spatial distribution of microfracturing in rock, *Geophys. J. R. Astron. Soc.*, *90*, 369–374.

Kagan, Y., and L. Knopoff (1978), Statistical study of the occurrence of shallow earthquakes, *Geophys. J. R. Astron. Soc.*, *55*, 67–86.

Kagan, Y., and L. Knopoff (1980), Spatial distribution of earthquakes: The two-point correlation function, *Geophys. J. R. Astron. Soc.*, *62*, 303–320.

Kurthz, J., and H. Herzel (1987), An attractor in solar time series, *Physica*, *25D*, 165–172.

Lay, T., and T. Wallace (1995), *Modern Global Seismology*, 521 pp., Academic, San Diego, Calif.

Lee, W., R. Bennett, and K. Meagher (1972), A method of estimating magnitudes of local earthquakes from signal duration, *U.S. Geol. Surv. Open File Rep.*, *28*.

Legrand, D., A. Cisternas, and L. Dorbath (1996), Multifractal analysis of the 1992 Erzincan aftershock sequence, *Geophys. Res. Lett.*, *23*, 933–936.

Legrand, D., A. Calahorrano, B. Guillier, L. Rivera, M. Ruiz, D. Villagómez, and H. Yepes (2002), Stress tensor analysis of the 1998–1999 tectonic swarm of northern Quito related to the volcanic swarm of Guagua Pichincha volcano, Ecuador, *Tectonophysics*, *344*, 15–36.

Main, I. (2000), Apparent breaks in scaling in the earthquake cumulative frequency-magnitude distribution: Fact or artifact?, *Bull. Seismol. Soc. Am.*, *90*, 86–97.

Matsumura, S., T. Ohkubo, and M. Imoto (1991), Seismic swarm activity in and around the Izu Peninsula preceding the volcanic eruption of July 13, 1989, *J. Phys. Earth*, *39*, 93–106.

Mogi, K. (1962), Magnitude-frequency relation for elastic shocks accompanying fractures of various materials and some related problems in earthquakes, *Bull. Earthquake Res. Inst. Univ. Tokyo*, *40*, 831–853.

Mogi, K. (1963), Some discussions on aftershocks, foreshocks, and earthquake swarms- The fracture of a semi-infinite body caused by an inner stress origin and its relation to the earthquake phenomena, 3, *Bull. Earthquake Res. Inst. Univ. Tokyo*, *41*, 615–658.

Mogi, K. (1969), Some features of recent seismic activity in and near Japan (2) Activity before and after great earthquakes, *Bull. Earthquake Res. Inst. Univ. Tokyo*, *47*, 395–417.

Ogata, Y. (1988), Statistical models for earthquakes occurrences and residual analysis for point processes, *J. Am. Stat. Assoc.*, *83*, 9–27.

Pacheco, J., C. Scholz, and L. Sykes (1992), Changes in frequency-size relationship from small to large earthquakes, *Nature*, *355*, 71–73.

Poupinet, G., W. Ellsworth, and J. Fréchet (1984), Monitoring velocity variations in the crust using earthquake doublets: An application to the Calaveras fault, California, *J. Geophys. Res.*, *89*, 5719–5731.

Power, J., M. Wyss, and J. Latchman (1998), Spatial variations in the frequency-magnitude distribution of earthquakes at Soufriere Hills volcano, Montserrat, West Indies, *Geophys. Res. Lett.*, *25*, 3653–3656.

Radulian, M., and C. Trifu (1991), Would it have been possible to predict the 30 August 1986 Vrancea earthquake?, *Bull. Seismol. Soc. Am.*, *81*, 2498–2503.

Rivera, L. (1989), Inversion du tenseur des contraintes et des mécanismes au foyer à partir des données de polarités pour une population de séismes. Application à l'étude du foyer de sismicité intermédiaire de Bucaramanga (Colombie), Thèse de doctorat, 266 pp., Univ. Strasbourg, Strasbourg, France.

Scholz, C. (1968), The frequency-magnitude relation of microfracturing in rock and its relation to earthquakes, *Bull. Seismol. Soc. Am.*, *58*, 399–415.

Scholz, C. (1982), Scaling laws for large earthquakes: Consequences for physical models, *Bull. Seismol. Soc. Am.*, *72*, 1–14.

Segovia, M. (2001), El sismo de Bahía del 4 de Agosto de 1998: Caracterización del mecanismo de ruptura y analisis de la sismicidad en la zona Costera, Diploma Ingeniero, 136 pp., Escuela Politécn. Nac., Quito, Ecuador.

Shimazaki, K. (1986), Small and large earthquakes: The effects of the thickness of seismogenic layer and the free surface, in *Earthquake Source Mechanics*, *Geophys. Monogr. Ser.*, vol. 37, pp. 209–216, AGU, Washington, D. C.

Simpson, D., W. Leith, and C. Scholz (1988), Two types of reservoir-induced seismicity, *Bull. Seismol. Soc. Am.*, *78*, 2025–2040.

Smith, W. (1981), The *b*-value as an earthquake precursor, *Nature*, *289*, 136–139.

Sornette, A., and D. Sornette (1999), Renormalization of earthquake aftershocks, *Geophys. Res. Lett.*, *26*, 1981–1984.

Spence, W. (1980), Relative epicenter determination using *P*-wave arrival time differences, *Bull. Seismol. Soc. Am.*, *70*, 171–183.

Suyehiro, S., T. Asada, and M. Ohtake (1964), Foreshocks and aftershocks accompanying a perceptible earthquake in central Japan, *Pap. Meteorol. Geophys.*, *15*, 17–88.

Sykes, L. (1970), Earthquake swarm and sea-floor spreading, *J. Geophys. Res.*, *75*, 6598–6611.

Villagómez, D. (2000), Sismicidad del volcán Guagua Pichincha, 1998–1999, Escuela Politécnica Nacional, facultad de geología, minas y petróleos, tesis de ingeniero geólogo, 114 pp., Escuela Politécn. Nac., Quito Univ., Quito, Ecuador.

Villagómez, D., M. Ruiz, H. Yepes, M. Hall, B. Guillier, A. Alvarado, M. Segovia, and A. Calahorrano (1999), Seismic activity at Guagua Pichincha volcano, Ecuador, Fourth International Symposium on Andean Geodynamics, Int. Lithosphere Program, Goettingen, Germany.

Volant, P., J. R. Grasso, J. L. Chatelain, and M. Frogneux (1992), *b*-value, aseismic deformation and brittle failure within an isolated geological object: Evidences from a dome structure loaded by fluid extraction, *Geophys. Res. Lett.*, *19*, 1149–1152.

Warren, N., and G. Latham (1970), An experimental study of thermally induced microfracturing and its relation to volcanic seismicity, *J. Geophys. Res.*, *75*, 4455–4464.

Wesnousky, S. (1999), Crustal deformation processes and the stability of the Gutenberg-Richter relationship, *Bull. Seismol. Soc. Am.*, *89*, 1131–1137.

Wiemer, S., and S. McNutt (1997), Variations in the frequency-magnitude distribution with depth in two volcanic areas: Mount St. Helens, Washington, and Mt. Spurr, Alaska, *Geophys. Res. Lett.*, *24*, 189–192.

Wiemer, S., and M. Wyss (1997), Mapping the frequency-magnitude distribution in asperities: An improved technique to calculate recurrence times?, *J. Geophys. Res.*, *102*, 15,115–15,128.

Wiemer, S., S. McNutt, and M. Wyss (1998), Temporal and three-dimensional spatial analyses of the frequency-magnitude distribution near Long Valley Caldera, California, *Geophys. J. Int.*, *134*, 409–421.

Wyss, M. (1973), Towards a physical understanding of the earthquake frequency distribution, *Geophys. J. R. Astron. Soc.*, *31*, 341–359.

Wyss, M., and R. Habermann (1988), Precursory seismic quiescence, *Pure Appl. Geophys.*, *126*, 319–332.

Wyss, M., K. Shimazaki, and S. Wiemer (1997), Mapping active magma chambers by b-value beneath Off-Izu volcano, Japan, *J. Geophys. Res.*, *102*, 20,413–20,433.

A. Calahorrano, Géosciences Azur, BP 48, F-06235 Villefranche-sur-Mer Cedex, France.

D. Legrand, Departamento de Geofísica (DGF), Universidad de Chile, Blanco Encalada 2085, Santiago, Chile. (denis@dgf.uchile.cl)

D. Villagómez, Department of Geological Sciences, 1272 University of Oregon, Eugene, OR 97405, USA.

H. Yepes, Instituto Geofísico de la Escuela Politécnica Nacional, apartado 2759, Quito, Ecuador.